Effect of Fiber Volume Fraction, Fiber Length and Fiber Tow Size on the Energy Absorption of Chopped Carbon Fiber–Polymer Composites

George C. Jacob
Materials Science and Engineering Department, University of Tennessee–Knoxville, 434 Dougherty Engineering, Knoxville, Tennessee 37996

J. Michael Starbuck
Polymer Matrix Composites Group, Metals and Ceramics Division, Oak Ridge National Laboratory, P.O. Box 2009, Oak Ridge, Tennessee 37831-8048

John F. Fellers
Materials Science and Engineering Department, University of Tennessee–Knoxville, 608 Dougherty Engineering, Knoxville, Tennessee 37996

Srdan Simunovic
Computational Material Science, Computer Science and Mathematics Division, Oak Ridge National Laboratory, P.O. Box 2008, Bldg. 6025, MS-6359, Oak Ridge, Tennessee 37831-6359

Composite materials have the potential to reduce the overall cost and weight of automotive structures with the added benefit of being able to dissipate large amounts of impact energy by progressive crushing. To identify and quantify the energy-absorbing mechanisms in candidate automotive composite materials, modified test methodologies were developed for conducting progressive crush tests on flat-plate composite specimens. The test method development and experimental setup focused on isolating the damage modes associated with the frond formation that occurs in dynamic testing of composite tubes. The Automotive Composites Consortium (ACC) is interested in investigating the use of chopped carbon fiber–reinforced composites as crash-energy absorbers primarily because the low costs involved in their manufacture make them cost-effective for automotive applications. While many in the past have investigated the energy-absorption characteristics in various continuous fiber–reinforced composite materials, no literature is available on the energy-absorption and crushing characteristics of chopped carbon fiber–reinforced composite materials. Hence quasi-static progressive crush tests were performed on composite plates manufactured from chopped carbon fiber (CCF) with an epoxy resin system using compression-molding techniques, and the effect of material parameters (fiber volume fraction, fiber length, and fiber tow size) on energy absorption was evaluated by varying them during testing. Of the parameters evaluated, fiber length appeared to be the most critical material parameter determining the specific energy absorption of a composite material, with shorter fibers having a higher specific energy absorption than longer fibers, possibly because of the increased concentration of stress raisers in the shorter fiber specimens, resulting in a larger number of fracture-initiation sites. The combination of material parameters that yielded the highest energy-absorbing material was identified. The test observations and trends established from this work would help support the development of low-cost energy absorbers for the automotive industry. POLYM. COMPOS., 26: 293–305 2005. Published 2005 Society of Plastics Engineers*

Correspondence to: G.C. Jacob; e-mail: gjacob@utk.edu
Contract grant sponsor: U.S. Department of Energy, Assistant Secretary for Energy Efficiency and Renewable Energy, Office of Transportation Technologies, Lightweight Materials Program; contract grant number: DE-AC05-00OR22725 (with UT-Battelle, LLC).

DOI 10.1002/pc.20100
Published online in Wiley InterScience (www.interscience.wiley.com).
Published 2005 Society of Plastics Engineers

INTRODUCTION

In passenger vehicles the ability to absorb impact energy and be survivable for the occupant is called the "crashworthiness" of the structure. This absorption of energy is through controlled failure mechanisms and modes that enable the maintenance of a gradual decay in the load profile. The crashworthiness of a material is expressed in terms of its specific energy absorption, SEA, which is defined as the energy absorbed per unit mass of crushed material.

Specific energy absorption, SEA, is dependent on many parameters, such as fiber type, matrix type, fiber orientation, specimen geometry, and fiber volume fraction. Changes in these parameters can cause subsequent changes in the specific energy absorption of composite materials up to a factor of 2. An important finding while investigating the effect of fiber type [1–16] on energy absorption is that a decrease in the density of the fiber causes an increase in the specific energy absorption. Fibers with high strain to failure result in greater energy absorption in the fiber-reinforced tubes. Studies on the effect of matrix type [6, 17–20] found higher energy-absorption capabilities with increase in the interlaminar fracture toughness of the thermoplastic matrix material. However, studies on fiber-reinforced thermoset composites found no dependence of specific energy upon resin fracture toughness, but there was a linear dependence upon the resin tensile strength and modulus [21]. Investigations on the dependence of fiber orientations [1, 2, 9, 17, 22–24] on energy absorption revealed fiber orientations that enhance the energy-absorption capability of composite materials require them to increase the number of fractured fibers, increase the material deformations, and increase the axial stiffness of the composite material and the lateral support to the axial fibers. Findings on the effect of specimen geometry [3, 7, 25–35] concluded that SEA follows the order: circular $>$ square $>$ rectangle, for a given fiber lay-up and tube geometry. Studies on the effect of fiber volume fraction [2, 22, 36–39] suggested an increase in fiber content would not always, as one would normally think, improve the energy-absorption capability of a composite material.

In the crashworthiness of automotive structures, the primary issues to the automotive industry are the overall economy and the weight of the material. To reduce the weight and improve the fuel economy, polymer composite materials have replaced more and more metal parts in vehicles. The tailorability of composites, in addition to their attributes of high strength-to-weight and stiffness-to-weight ratios, corrosion resistance and fatigue resistance, makes them very attractive for designing crashworthy structures. The challenge is to determine what specific design features are needed in the geometry and what material systems will enable greater safety without negatively affecting the overall economics of fabrication and production.

In comparison to metals, most composites are generally characterized by a brittle rather than ductile response to the applied loads, especially in compression. The major difference, however, is that metal structures collapse under crush or impact by buckling and/or folding in accordion-type fashion involving extensive plastic deformation, whereas composites fail through a sequence of fracture mechanisms. The actual mechanisms, e.g., fiber fracture, matrix crazing and cracking, fiber-matrix debonding, delamination, and inter-ply separation, and sequence of damage are highly dependent on lamina orientation, crush speed, triggers and geometry of the structure.

Much of the experimental work to study the energy absorption of composite materials has been carried out on axisymmetric tubes. Tube structures are relatively easy to fabricate and close to the geometry of the actual crashworthy structures. These tubes were designed to absorb impact energy in a controlled manner by providing a trigger to initiate progressive crushing. The most widely used method of triggering is chamfering one end of the tube.

Both material and structural damage processes need to be well understood to accurately model and design crashworthy automotive composite structures. In the progressive crushing of composite tubes, many different failure mechanisms contribute to the overall energy absorption of the structure. Chopped carbon-fiber composite plate specimens were tested using a unique test fixture to isolate the damage mechanisms and quantify the effect of material variables like fiber tow size, fiber length and fiber volume fraction on the CCF composite's energy absorption. The design is a modified version of an existing test fixture used for crush testing of composite plates [40].

There are some published works on different designs of plate fixtures in the literature. Test fixtures designed by Lavoie and Morton [40], Fleming and Vizzini [41] and Daniel et al. [42] could accommodate wide specimens that were fully supported to prevent specimen buckling but had a flat crush profile. In order to initiate progressive crushing and simulate the damage modes associated with frond formation that occurs in dynamic testing of composite tubes, different contact profile blocks having radii 6.4 mm (0.25 inch) and 13 mm (0.5 inch) respectively and a frictionless roller for constraining the specimen to deform along the path of the contact profile were incorporated into a new plate test fixture design [43]. Though the test fixture designed by Yuan and Viegelahn [44] was simple and had a bent crush profile, it suffered from large frictional effects.

Practical considerations related to the cost of production of the test specimens were of paramount importance in developing the test methodology. Composite plate specimens are very cheap to fabricate, and it has been observed that plate specimens progressively crush in modes very similar to the damage modes that occur during progressive crushing of composite tubes. Also plates can be easily produced with consistently high quality.

EXPERIMENTAL

Material System Investigated: Chopped Carbon Fiber/Epoxy Resin System

Ongoing research programs have generated a considerable amount of experimental data related to the energy-absorption characteristics of polymer composite materials. For this class of materials the energy absorption is depen-

TABLE 1. CCF tensile strength.

Panel group	Fiber tow size	Fiber volume fraction	Fiber length
CCF1	150gsm (12K)	40%	1 inch
CCF2	150gsm (12K)	40%	2 inches
CCF3	300gsm (48K)	40%	2 inches
CCF5	150gsm (12K)	50%	1 inch
CCF6	150gsm (12K)	50%	2 inches
CCF7	300gsm (48K)	50%	2 inches
CCF8	300gsm (48K)	40%	1 inch
CCF9	300gsm (48K)	50%	1 inch

dent on many parameters, including fiber type, matrix type, fiber architecture, specimen geometry, processing conditions, fiber volume fraction, and impact velocity. Changes in these parameters can cause subsequent changes in their specific energy absorption up to a factor of 2. Composite materials are recognized as being efficient energy absorbers; however, for a material to be suitable for automotive crashworthy structural applications, it must also have low raw material and manufacturing costs. The use of chopped carbon fiber and compression-molded processing methods has the potential to satisfy these criteria. Hence the ACC (Automotive Composites Consortium) was interested in investigating the use of carbon fibers in chopped fiber–reinforced composite materials. Carbon fiber–reinforced tubes display higher specific energy absorption than other fiber-reinforced tubes. This is a direct result of the lower density of the carbon fiber, which thus also contributes to the light weight of the structures in which they are used. Epoxy, regarded as a standard resin that frequently finds use in composites, was chosen as the matrix.

The chopped carbon fiber composite plates were manufactured from Toray T700 chopped carbon fiber with YLA RS-35 epoxy resin using compression-molding techniques. YLA Incorporated supplied the molding compound; CCS Composites LLC compression-molded the plates.

Variables Investigated

An attempt was made to understand in detail the effect the material parameters (fiber volume fraction, fiber length and fiber tow size) have on the energy-absorption characteristics of chopped carbon-fiber composite plates. The following is a summary of the various material variables that were investigated: tow size: 48K (300 gsm), 12K (150 gsm); fiber volume fraction: 50%, 40%; fiber length: 1, 2 inches.

Eight-panel groups of compression-molded chopped carbon fiber/epoxy composites were fabricated; the fiber length, fiber volume fraction and fiber areal density were varied. The different fiber lengths were 1 inch and 2 inches, the different fiber volume fractions were 40% and 50%, and the areal density was either 150 gsm or 300 gsm. Different areal densities were evaluated in an attempt to study the effect of tow size. The Toray T700 fiber used for the prepreg was a 12K tow but in manufacturing the molding compound the prepreg was slit in addition to cutting the length. The width of the slit was varied to provide the different areal densities. Descriptions of the various panel groups are given in Table 1.

Test Method

A new test fixture design was developed for determining the deformation behavior and damage mechanisms that occur during progressive crushing of composite plates [43]. Features incorporated into the design include an observable crush zone, long crush length (2 inches), interchangeable contact profile, frictionless roller for contact constraint, and out-of-plane roller supports to prevent buckling.

The composite plate specimen is clamped in the top plate by the grip inserts. The specimen is then loaded in compression and crushed through the contact profile as defined by the profile block via the top plate that is connected to the load train using a shaft coupler. The top plate is displaced downward, relative to the base plate and profile block. Alignment is maintained by using four linear shafts and linear bearings. Attached to the roller plates that are positioned on the linear shafts by shaft collars are the roller ways. The roller ways are used to reduce the unsupported length of the specimen thereby preventing the specimen from buckling. The brackets on either side of the profile plate were designed to provide a method of constraining the specimen to deform along the path of the contact profile. Using oil-impregnated bronze sleeve bearings in each bracket and installing a precision ground shaft that acts as a roller accomplish this. The severity of the contact profile

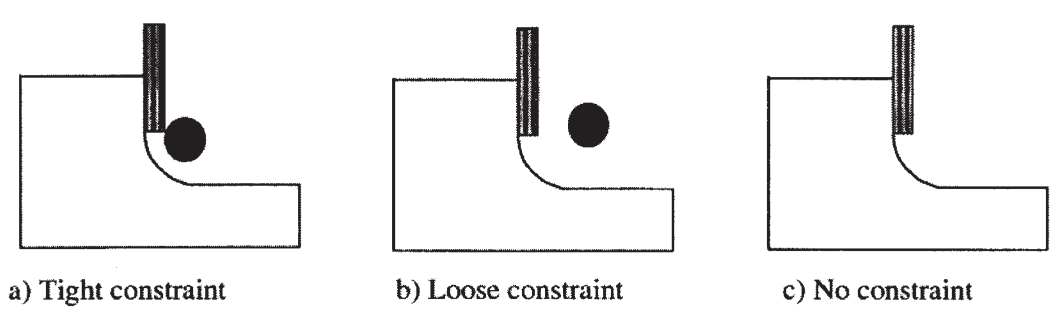

FIG. 1. Constraint conditions.

TABLE 2. CCF tensile strength.

Panel type	ID	Max. stress (ksi) Avg.	Max. stress (ksi) C.V.	Max. strain (%) Avg.	Max. strain (%) C.V.	Stiffness (Msi) Avg.	Stiffness (Msi) C.V.
40% Vf, 1-in., 150 gsm	CCF1	29.4	23.8	0.42	11.90	7.08	19.63
40% Vf, 1-in., 300 gsm	CCF8	23.0	5.2	0.43	34.88	5.49	34.06
40% Vf, 2-in., 150 gsm	CCF2	51.6	18.8	0.58	5.17	9.04	23.67
40% Vf, 2-in., 300 gsm	CCF3	20.8	36.5	0.28	42.86	6.77	1.33
50% Vf, 1-in., 150 gsm	CCF5	28.3	16.6	0.46	10.87	6.06	13.86
50% Vf, 1-in., 300 gsm	CCF9	20.8	18.8	0.48	33.33	4.67	50.96
50% Vf, 2-in., 150 gsm	CCF6	46.4	10.6	0.61	9.84	7.79	4.24
50% Vf, 2-in., 300 gsm	CCF7	23.8	8.0	0.48	47.92	5.26	28.71

constraint is determined by the position of the load cell brackets and is adjustable using slotted positioning holes (see Fig. 1). Slotted holes are used throughout the test fixture design to accommodate different plate thicknesses and maintain alignment with the centerline of the load train.

Quasi-static progressive crush tests (3 replicates at each condition) were performed on the CCF composite plates. The CCF specimens had a nominal length of 178 mm (7 inches), thickness of 3 mm (0.13 inch) and a width of 50 mm (2 inches), 25.4 mm (1 inch), or 13 mm (0.5 inch) and a 45° chamfer was used as the crush initiator. In some of the tests a metal push plate was used to reduce the unsupported specimen length. This metal push plate was 76 mm (3 inches) in length and was bonded to the end of the test specimen using 5-minute epoxy. This called for the test specimen to be trimmed to a length of 102 mm (4 inches) so that it could accommodate the metal push plate. A servo-hydraulic test machine and a loading rate of 5 mm/min (0.2 inch/min) were used throughout the entire testing. The load-deflection response was recorded using a computerized data acquisition system. Specific energy absorption, $SEA = W/(AL\rho)$, was used to calculate the specific energy absorption of the composite plate specimens tested, where 'W' is the total energy absorbed in crushing of the specimen, which is the area under the load-displacement curve, 'ρ' is the density of the composite material, 'A' and 'L' are the cross-sectional area and length of the crushed portion of the composite plate specimen, respectively. The energy absorbed during initiation before stable progressive crushing takes place is omitted in the calculation of the SEA as a means of achieving a sustained crushing behavior characteristic.

MECHANICAL PROPERTIES

Characterization tests were conducted to evaluate the tension, compression, and flexural mechanical properties of the eight different panel types. The tensile strength was evaluated using the ASTM D3039/D 3039M-95a with dog-bone specimen geometry and the strain was measured using an extensometer. Compression strength tests were run as per ASTM D3410/D3410M-95 (IITRI Method) and strain gauges were used for measuring strains. The flexural strength was determined based on ASTM D790-98 and 4-point loading with a span to depth ratio equal to 16. An LVDT was used for measuring the beam deflection. The test results are summarized in Tables 2, 3 and 4 based on a limited sample population (3 specimens per panel type for tension and compression, and 6 specimens for flexure).

Based on the results shown in Tables 2, 3 and 4, some observations from the mechanical property testing are as follows. The smaller the tow size of the CCF, the higher the tensile strength and the higher the tensile modulus. Lower tensile strengths and stiffnesses were measured when the chopped fiber length was shorter or when higher fiber volume fractions were used. From the compression tests, the smaller tow size panels had significantly higher compressive strengths and failure strains than the larger tow size

TABLE 3. CCF compressive strength.

Panel type	ID	Max. stress (ksi) Avg.	Max. stress (ksi) C.V.	Max. strain (%) Avg.	Max. strain (%) C.V.	Stiffness (Msi) Avg.	Stiffness (Msi) C.V.
40% Vf, 1-in., 150 gsm	CCF1	47.1	9.8	1.23	13.82	5.29	16.07
40% Vf, 1-in., 300 gsm	CCF8	30.0	10.0	0.77	31.17	4.96	14.52
40% Vf, 2-in., 150 gsm	CCF2	44.4	5.0	1.45	17.93	3.89	19.02
40% Vf, 2-in., 300 gsm	CCF3	36.2	3.9	0.70	5.71	5.70	0.88
50% Vf, 1-in., 150 gsm	CCF5	34.3	5.5	1.31	16.03	3.62	9.95
50% Vf, 1-in., 300 gsm	CCF9	27.9	15.8	0.65	63.08	5.44	38.60
50% Vf, 2-in., 150 gsm	CCF6	53.2	8.1	1.13	2.66	5.45	13.76
50% Vf, 2-in., 300 gsm	CCF7	32.0	19.1	0.80	23.75	4.78	36.19

TABLE 4. CCF 4-point flexure strength.

Panel type	ID	Max. stress (ksi)		Max. strain (%)		Stiffness (Msi)	
		Avg.	C.V.	Avg.	C.V.	Avg.	C.V.
40% Vf, 1-in., 150 gsm	CCF1	46.1	17.4	1.84	10.87	0.70	10.00
40% Vf, 1-in., 300 gsm	CCF8	30.5	20.0	1.51	21.19	0.60	11.67
40% Vf, 2-in., 150 gsm	CCF2	58.1	18.1	2.10	5.71	0.67	8.96
40% Vf, 2-in., 300 gsm	CCF3	37.8	26.2	1.63	15.95	0.58	24.14
50% Vf, 1-in., 150 gsm	CCF5	49.7	14.3	1.52	10.53	0.80	12.50
50% Vf, 1-in., 300 gsm	CCF9	38.2	17.0	1.33	25.56	0.76	14.47
50% Vf, 2-in., 150 gsm	CCF6	71.0	15.2	1.91	7.85	0.73	8.22
50% Vf, 2-in., 300 gsm	CCF7	36.9	14.4	1.70	17.65	0.56	8.93

panels. The effects of fiber length and fiber volume fraction on compressive strength, stiffness and maximum strain were inconclusive. Consistent with the tension and compression data, the flexure data indicates that testing smaller tow size panels results in higher strengths and stiffnesses. The effect of fiber volume fraction on the flexural response is opposite that of pure tension, where the higher fiber volume fraction tests resulted in higher flexural strengths and stiffnesses. The effect of fiber length was lower flexure strength and higher flexure stiffness when shorter lengths were tested. It should be noted that all the mechanical properties had tremendous scatter as indicated by the large coefficient of variations in the tables. This variability in the property data may be indicative of a nonhomogeneous material system and the lack of randomness of the chopped carbon fiber orientation.

RESULTS AND DISCUSSION OF THE PROGRESSIVE CRUSH TESTS

For all specimens tested, local crushing took place at the chamfered end of the plates. Matrix cracking occurred at the ends of the fiber tows due to stress concentration at these ends. Fiber-matrix debonding also took place in a majority of the specimens that were tested. Flexural deformations controlled the damage process. Some of the test specimens, when loaded in the no-constraint condition, experienced fiber pullout, fiber breakage in the tension side, and fiber buckling in the compression side of the specimen. The fracture mechanism that took place in specimens crushed in the loose- and tight-constraint condition was the same in all specimens, and the specimen failure was more or less predictable. On the contrary, the specimens that were crushed in the no-constraint condition fractured in rather erratic fashions, and specimen failure was far less predictable. This was due to absence of the much-needed roller constraint required to direct the crushing process. Some of the no-constraint tests led to catastrophic failure of the specimen where in the specimen broke into 2 or 3 pieces.

The specimens tested in the loose- and tight-constraint conditions generated load-deflection curves that were similar to the ones generated during the progressive crushing of composite tubes. It had 4 stages, the first being characterized by an initial rapid load increase. A rapid load drop

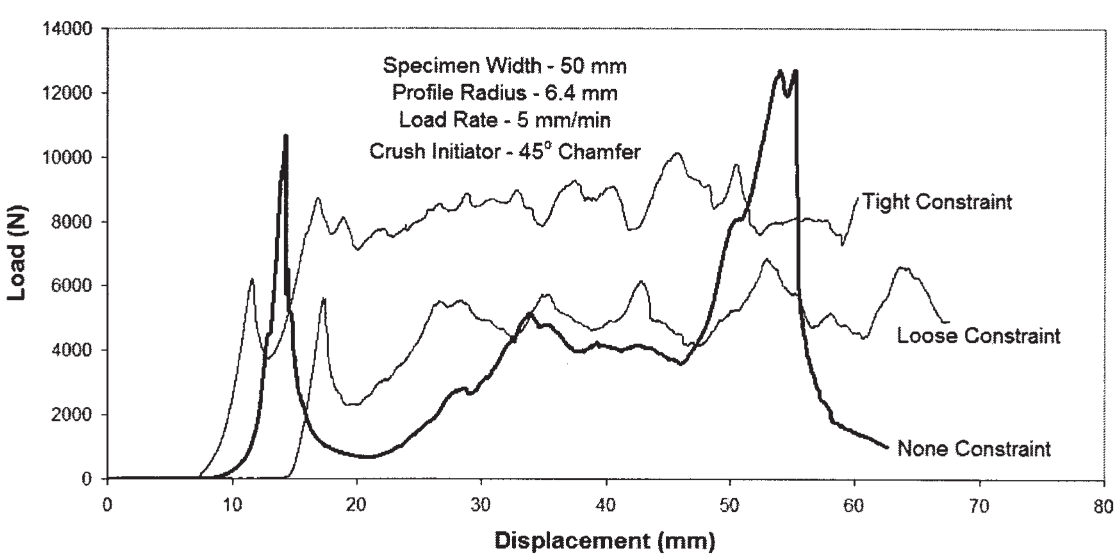

FIG. 2. Load-displacement traces for CCF.

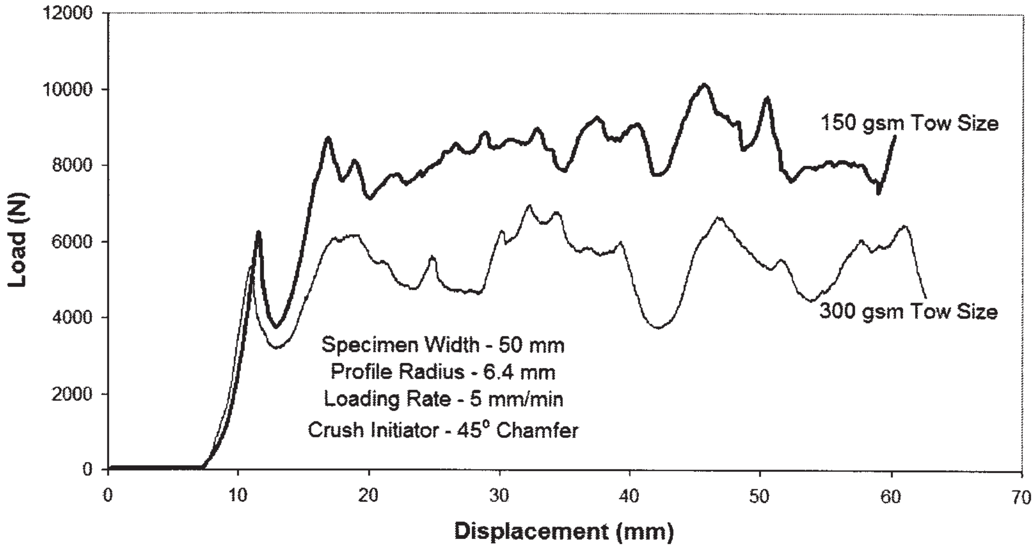

FIG. 3. Load-displacement traces representing the effect of tow size on the SEA of CCF with 1-inch fiber length.

occurred in the second stage of the load-deflection curve, followed by a gradual saturation of the load. The final stage was characterized by stable crushing at a constant mean load (see Fig. 2). The small load fluctuations and serrations in the fourth stage of the curve are characteristic of stable crushing.

Effect of Tow Size

Comparison of panel group CCF5 (150 gsm, 50% F.V., 1 inch F.L.) and panel group CCF9 (300 gsm, 50% F.V., 1 inch F.L.) revealed that the specific energy absorption of CCF5 was greater than that of CCF9. For a comparison of the load-displacement traces recorded for a test conducted on a specimen belonging to panel group CCF5 and on a specimen belonging to panel group CCF9, please see Fig. 3. Panel group CCF1 (150 gsm, 40% F.V., 1 inch F.L.) and panel group CCF8 (300 gsm, 40% F.V., 1 inch F.L.) were also compared; the specific energy absorption of CCF1 was greater than that of CCF8. From these results it was concluded that an increase in tow size caused a decrease in the specific energy absorption for chopped carbon-fiber com-

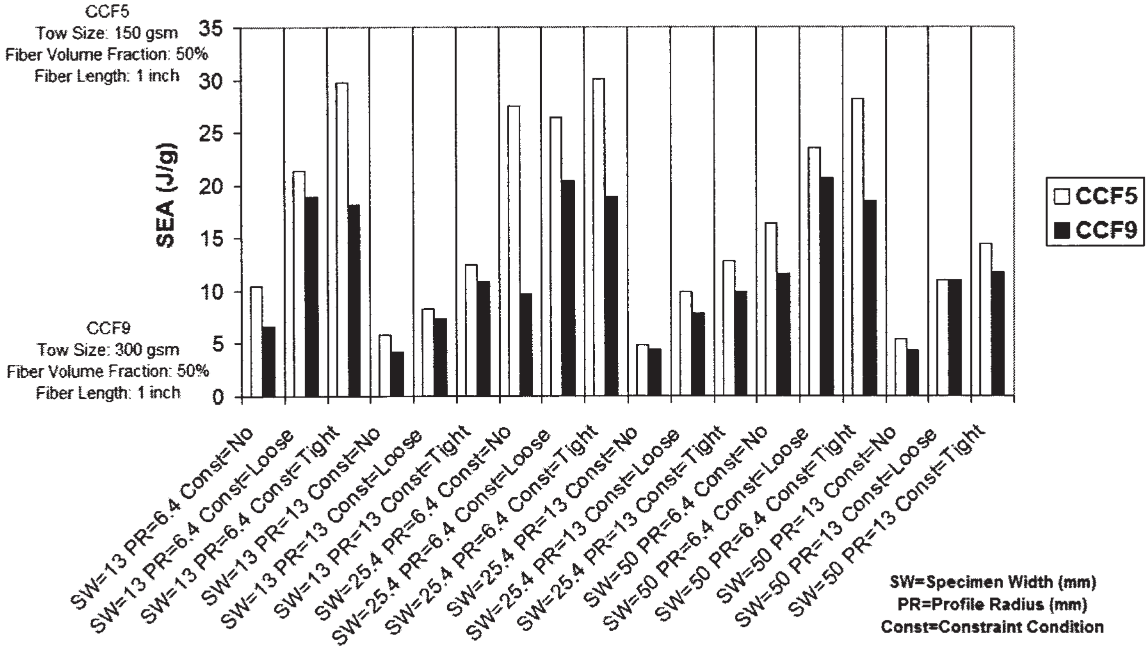

FIG. 4. Effect of tow size on the SEA of CCF with 1-inch fiber length and 50% fiber volume fraction.

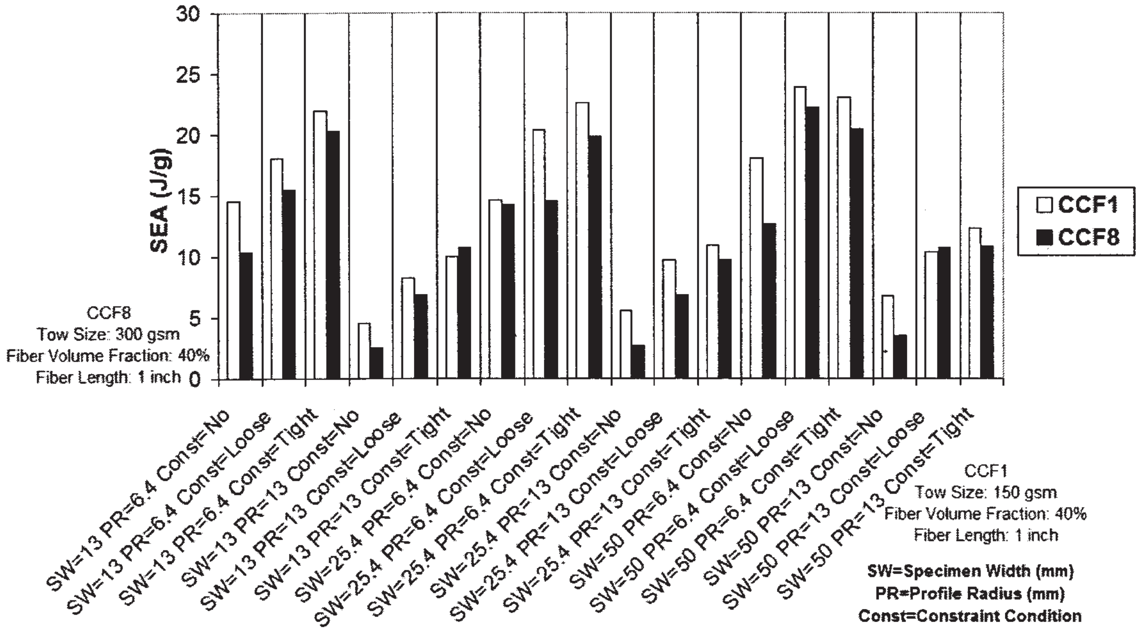

FIG. 5. Effect of tow size on the SEA of CCF with 1-inch fiber length and 40% fiber volume fraction.

posite materials with 1-inch fiber length (see Figs. 4 and 5). It could be the tow size that directly affects the observed behavior, or the toll of the artifacts that are produced during the manufacture of a larger tow imposes on the overall specimen condition. These artifacts might be a result of not being able to get the resin in between all the fibers or the incomplete filling of the voids.

However, the trends in the data were not as consistent for the 2-inch fiber length, and it was concluded that there was no serious effect of tow size for the longer fiber length.

Effect of Fiber Volume Fraction

Comparison of panel group CCF2 (150 gsm, 40% F.V., 2 inch F.L.) and panel group CCF6 (150 gsm, 50% F.V., 2 inch F.L.) revealed that the specific energy absorption of CCF2 was greater than that of CCF6. Panel group CCF3 (300 gsm, 40% F.V., 2 inch F.L.) and panel group CCF7 (300 gsm, 50% F.V., 2 inch F.L.) were also compared; the specific energy absorption of CCF3 was greater than that of CCF7. For a comparison of the load-displacement traces recorded for a test conducted on a specimen belonging to

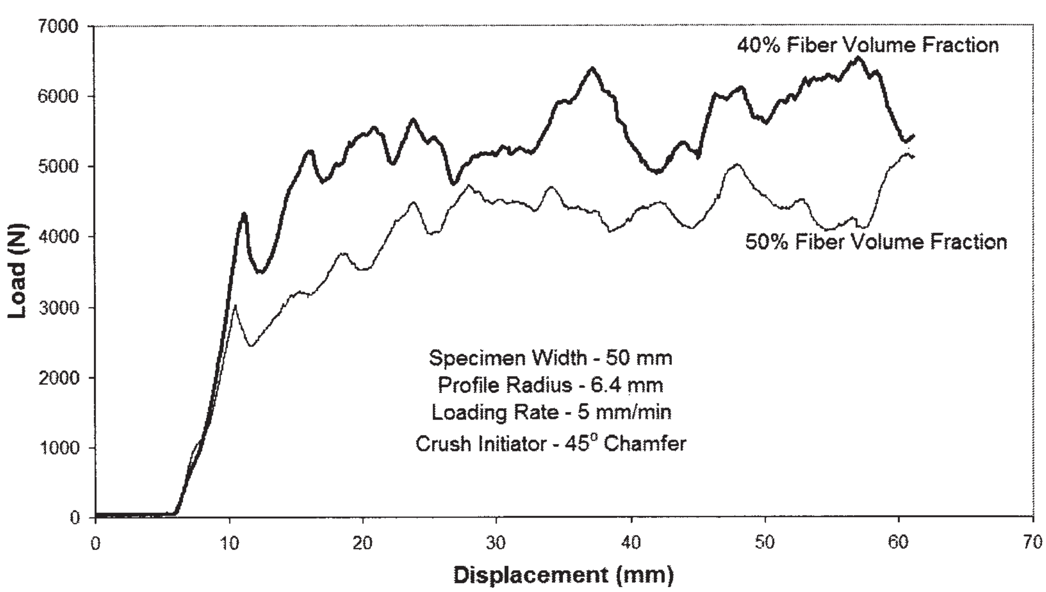

FIG. 6. Load-displacement traces representing the effect of fiber volume fraction on the SEA of CCF with 2-inch fiber length.

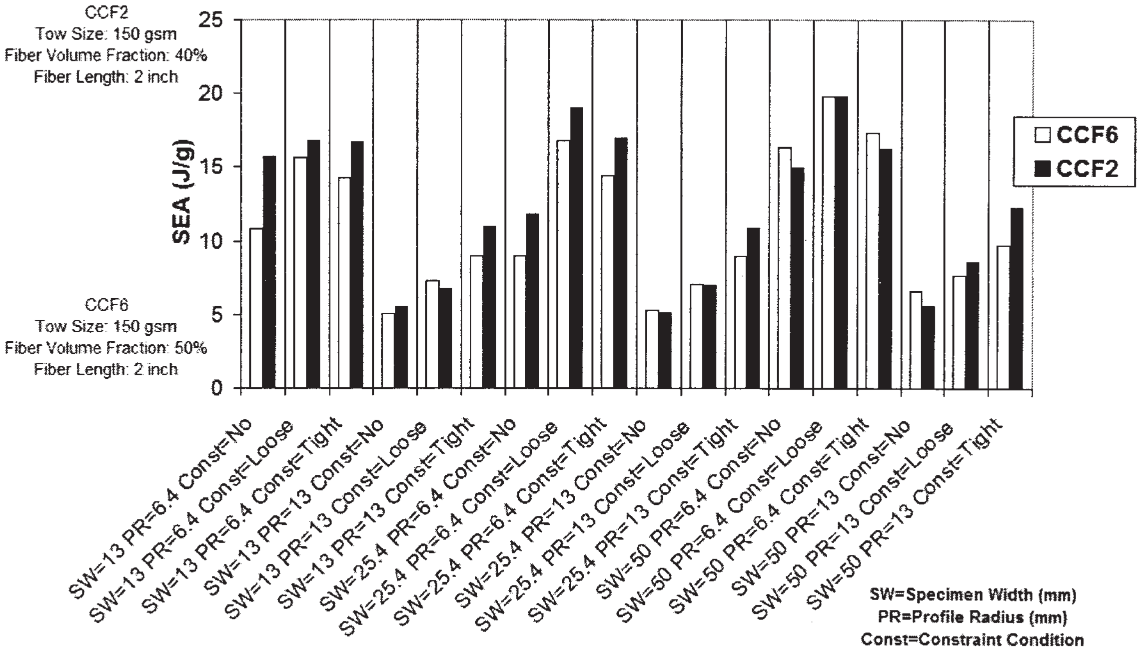

FIG. 7. Effect of fiber volume fraction on SEA of CCF with 2-inch fiber length and tow size 150 gsm.

panel group CCF3 and on a specimen belonging to panel group CCF7 (see Fig. 6). Hence it was concluded that an increase in fiber volume fraction caused a decrease in the specific energy absorption for chopped carbon-fiber composite materials with fiber length of 2 inches (see Figs. 7 and 8).

However, comparison of panel group CCF5 (150 gsm, 50% F.V., 1 inch F.L.) and panel group CCF1 (150 gsm, 40% F.V., 1 inch F.L.) revealed that the specific energy absorption of CCF5 was greater than that of CCF1. For a comparison of the load-displacement traces recorded for a test conducted on a specimen belonging to panel group CCF5 and on a specimen belonging to panel group CCF1 (see Fig. 9). From this data it was concluded that an increase in fiber volume fraction caused an increase in the specific energy absorption for chopped carbon-fiber composite materials with 1-inch fiber length (see Fig. 10).

It is not always true, as one would normally think, that an increase in the fiber content necessarily improves the spe-

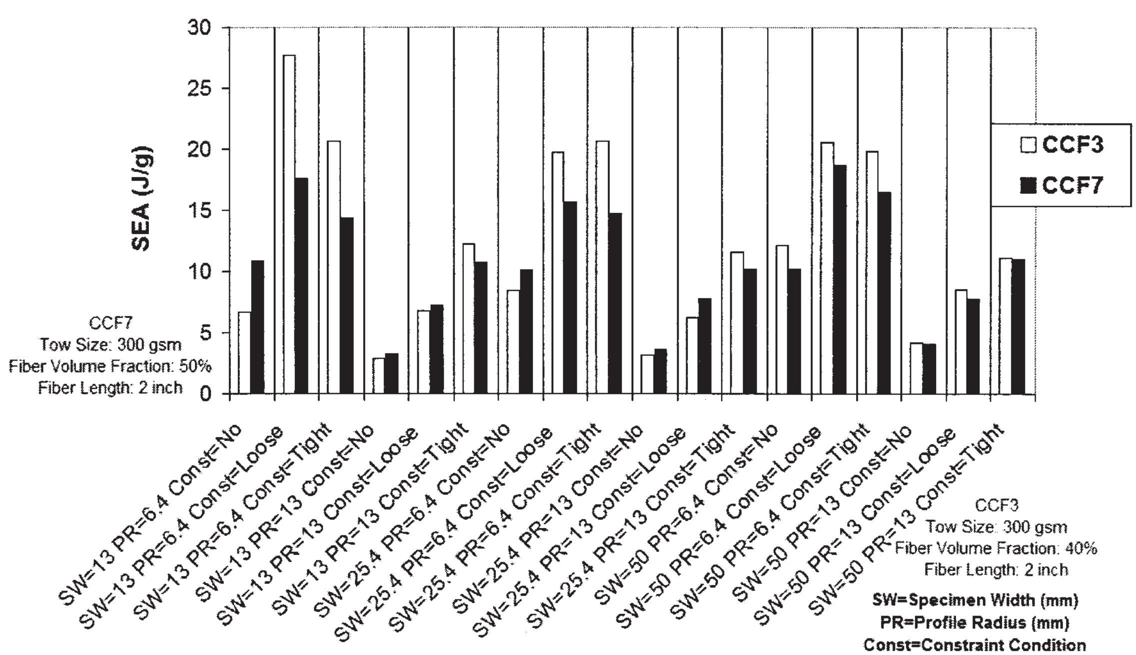

FIG. 8. Effect of Fiber Volume Fraction on SEA of CCF with 2-inch fiber length and tow size 300 gsm.

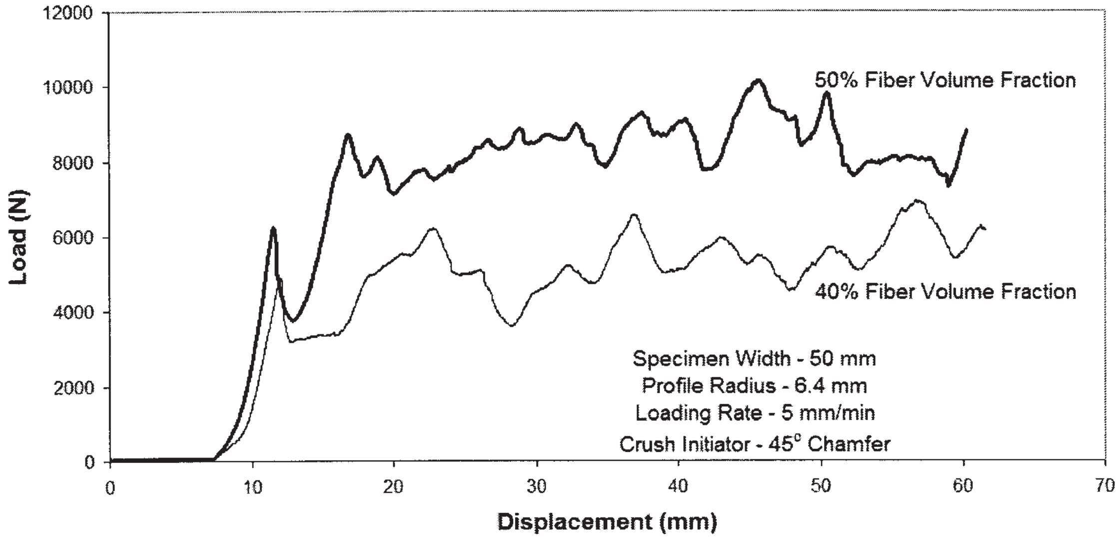

FIG. 9. Load-displacement traces representing the effect of fiber volume fraction on the SEA and CCF with 1-inch fiber length.

cific energy-absorption capability of a composite material. A possible explanation for this is that as the fiber volume fraction increases, the volume of the matrix between the fibers decrease. This causes an increase in the matrix density. This further leads to a decrease in the interlaminar strength of the composite. As interlaminar strength decreases, interlaminar cracks form at lower loads, resulting in a reduction in the energy-absorption capability.

Effect of Fiber Length

Comparison of panel group CCF5 (150 gsm, 50% F.V., 1 inch F.L.) and panel group CCF6 (150 gsm, 50% F.V., 2 inch F.L.) revealed that the specific energy absorption of CCF5 was greater than that of CCF6. For a comparison of the load-displacement traces recorded for a test conducted on a specimen belonging to panel group CCF5 and on a specimen belonging to panel group CCF6 (see Fig. 11). Panel group CCF1 (150 gsm, 40% F.V., 1 inch F.L.) and panel group CCF2 (150 gsm, 40% F.V., 2 inch F.L.) were also compared; the specific energy absorption of CCF1 was greater than that of CCF2. Therefore it was concluded that an increase in fiber length caused a decrease in the specific energy absorption for chopped carbon-fiber composite materials with 150-gsm tow size (see Figs. 12 and 13).

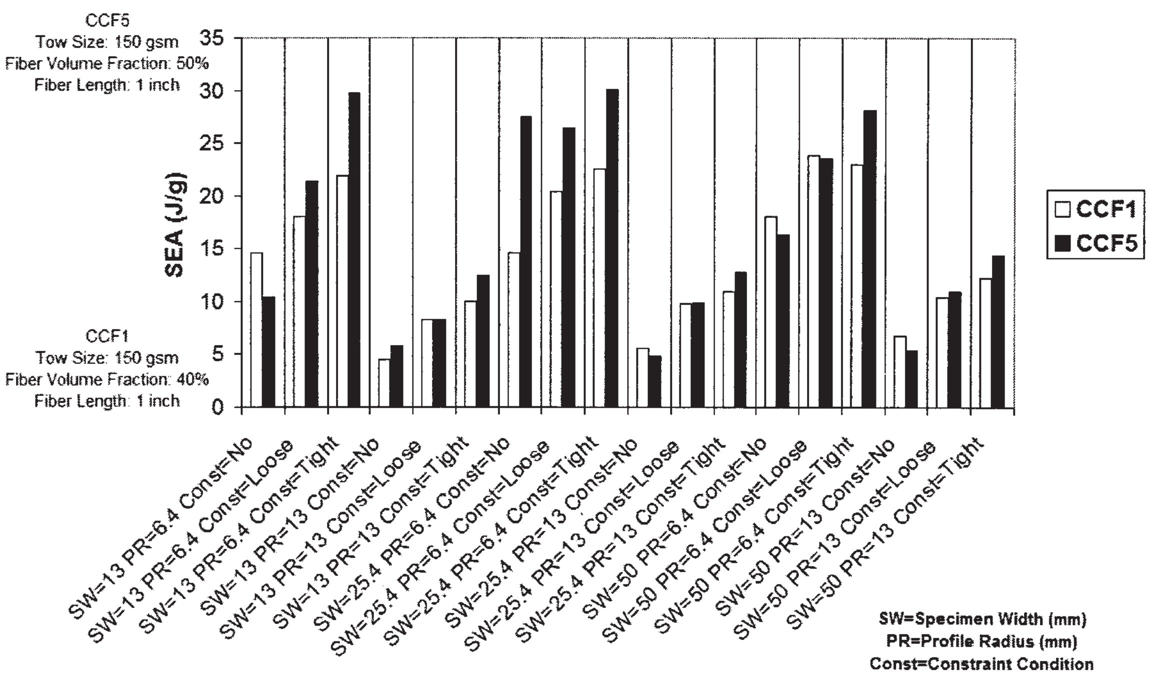

FIG. 10. Effect of fiber volume fraction on SEA of CCF with 1-inch fiber length and tow size 150 gsm.

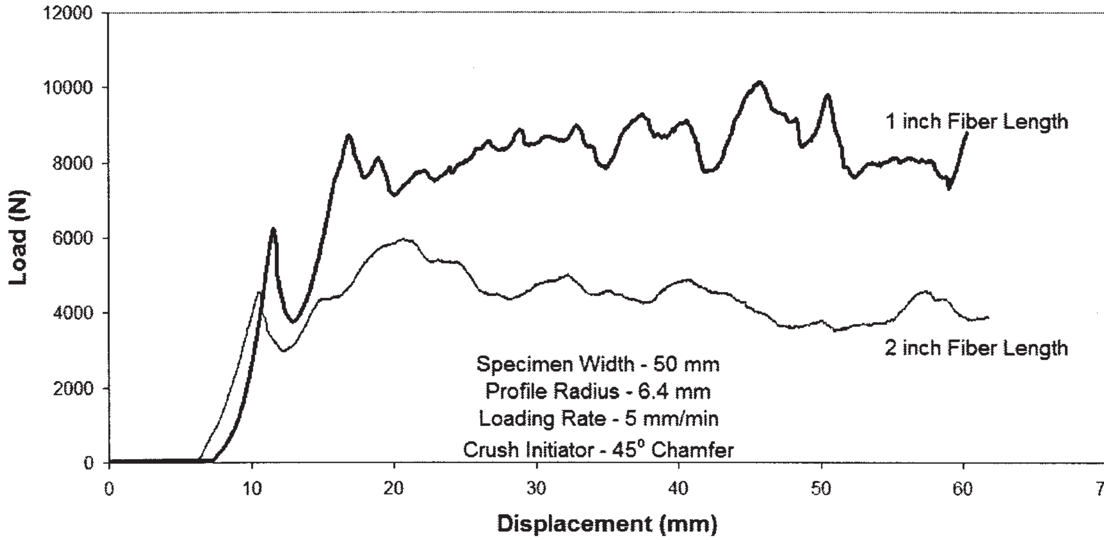

FIG. 11. Load-displacement traces representing the effect of fiber length on the SEA of CCF with 150 gsm tow size.

When panel group CCF9 (300 gsm, 50% F.V., 1 inch F.L.) and panel group CCF7 (300 gsm, 50% F.V., 2 inch F.L.) were compared, the specific energy absorption of CCF9 was greater than that of CCF7. For a comparison of the load-displacement traces recorded for a test conducted on a specimen belonging to panel group CCF9 and on a specimen belonging to panel group CCF7 (see Fig. 14). Hence it was concluded that an increase in fiber length caused a decrease in the specific energy absorption for chopped carbon-fiber composite materials with 300-gsm tow size (see Fig. 15).

Previous studies on the effect of fiber length on the energy-absorption capabilities of composites have reported an increase in the specific energy absorption, SEA, with increased fiber lengths [38], though the data was subjected to a considerable amount of scatter. The effect of fiber length on SEA observed in this work, that an increase in fiber length from 1 inch to 2 inches caused a decrease in the SEA for the CCF plates up to a factor of 2, disagrees with this observation. The specimen plates using 1-inch fibers have a relatively larger number of fiber ends than the plates having a fiber length of 2 inches. These fiber ends serve as stress raisers, resulting in a larger number of fracture-initiation sites in the specimens with 1-inch fiber length, thus

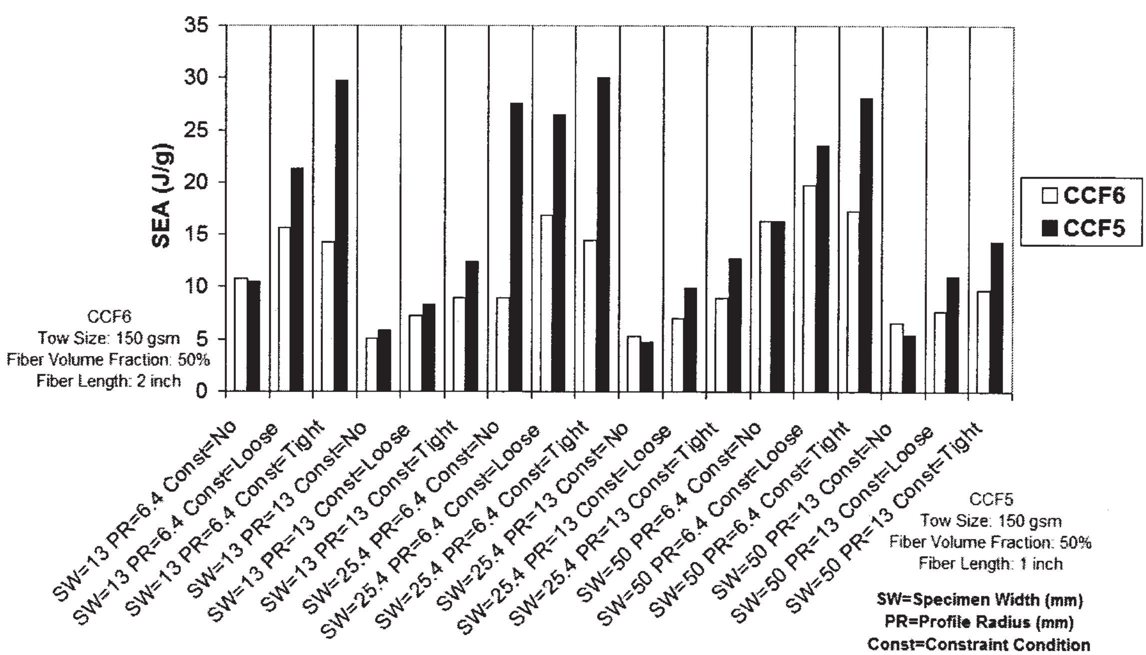

FIG. 12. Effect of fiber length on the SEA of CCF with 150 gsm tow size and 50% fiber volume fraction.

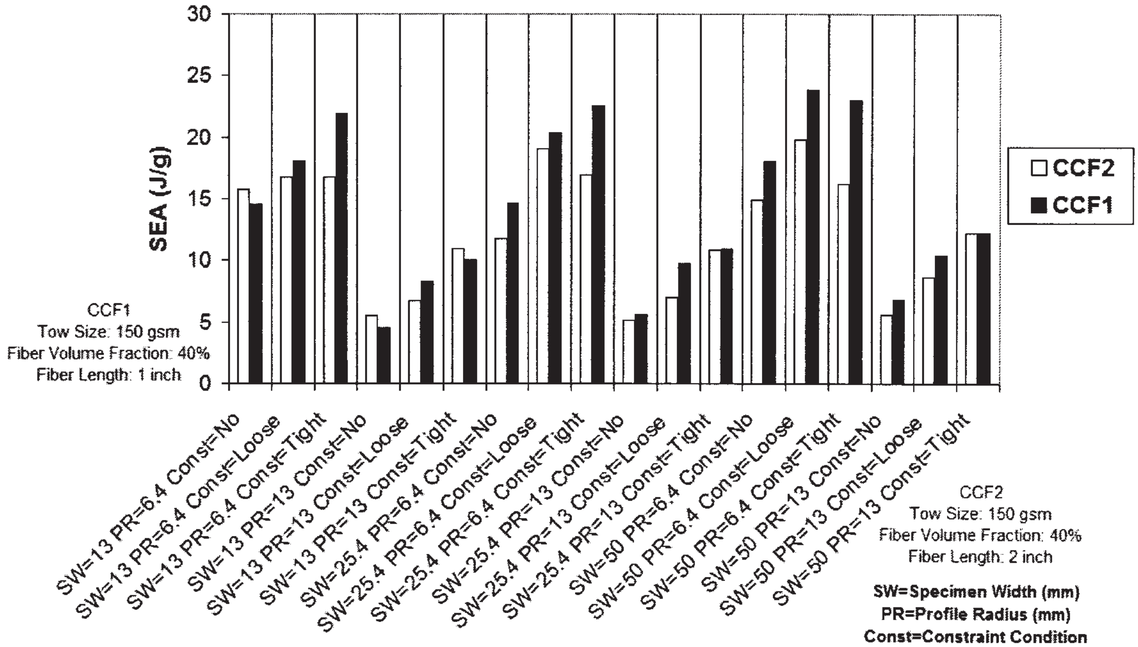

FIG. 13. Effect of fiber length on the SEA of CCF with 150 gsm tow size and 40% fiber volume fraction.

causing more matrix cracking and deformation and leading to a higher SEA.

Highest and Lowest Energy-Absorbing Panel Groups

The panel group having the highest SEA was CCF5 (150 gsm (12 K), 50% F.V., 1 inch F.L.). The two panel groups with the lowest SEA were CCF6 (150 gsm (12 K), 50% F.V., 2 inch F.L.) and CCF7 ((300 gsm (48 K), 50% F.V., 2 inch F.L.). The above results indicate that it is the 2-inch-long fibers that cause the SEA of the CCF6 and CCF7 panel groups to be the least among all the CCF panel groups. Further, the conclusion resulting from this work that an increase in fiber length causes a decrease in the SEA agrees with the above observation. Therefore it is concluded that fiber length appears to be the most critical material parameter determining the SEA of a composite material, with shorter fiber lengths leading to higher specific energy absorptions.

CONCLUSION

Quasi-static progressive crush strip tests were conducted on randomly oriented CCF composite materials to evaluate

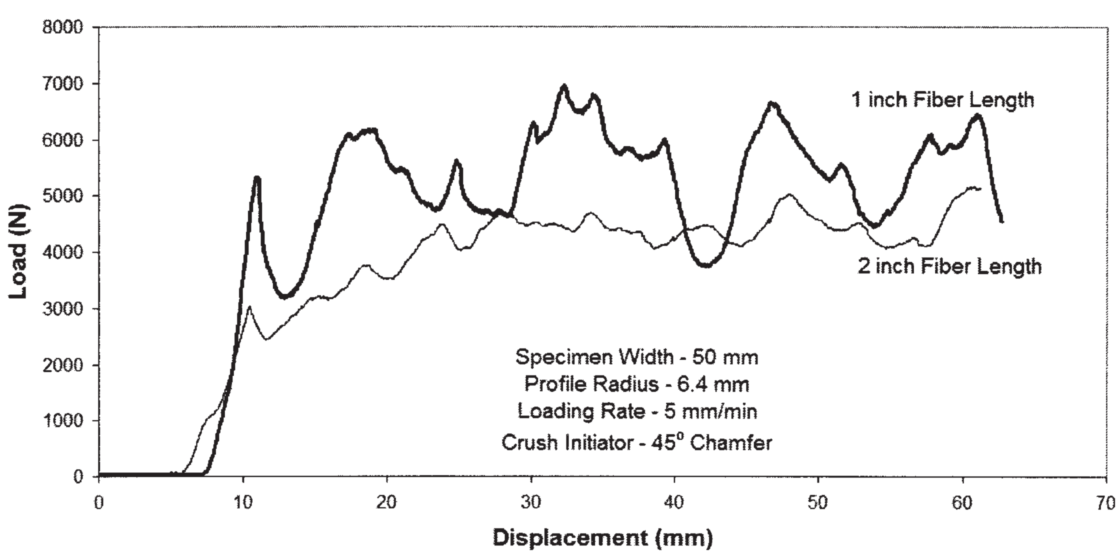

FIG. 14. Load-displacement traces representing the effect of fiber length on the SEA of CCF with 300 gsm tow size.

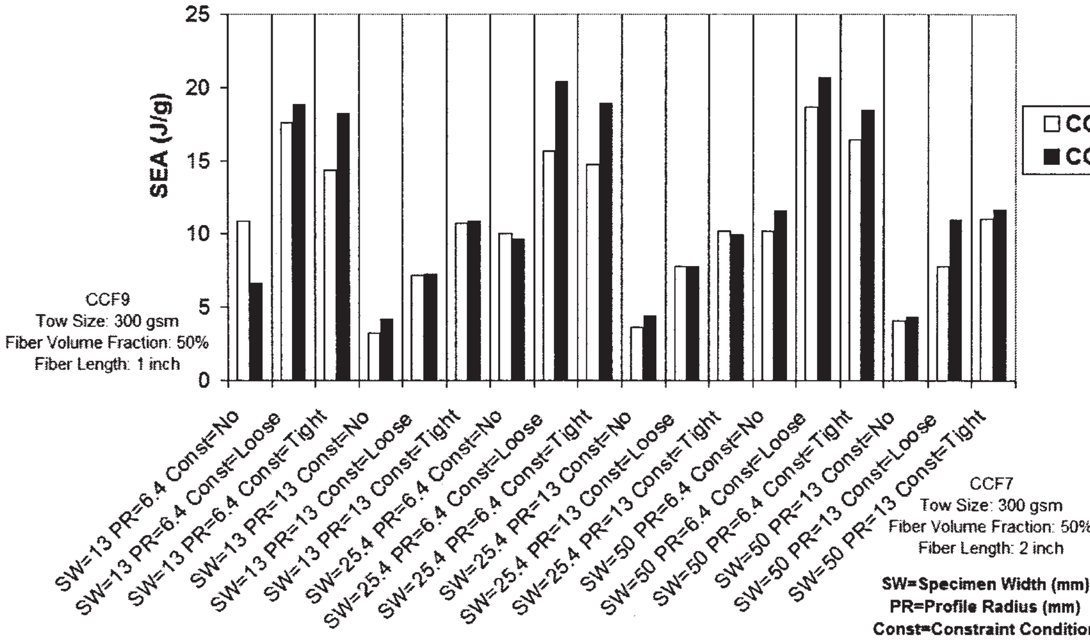

FIG. 15. Effect of fiber length on the SEA of CCF with 300 gsm tow size and 50% fiber volume fraction.

the effect of various material parameters (fiber volume fraction, fiber length and fiber tow size) on their energy-absorption capability. The objective of the test method was to simulate the frond formation observed during dynamic crush tests of composite tubes. Eight different types of panels were fabricated and tested, and the panel group having the highest SEA (CCF5) corresponded to 50% fiber volume fraction, 1-inch fiber length, and 150-gsm tow size. The two panel groups that recorded the lowest SEA were CCF6 (150 gsm fiber tow size, 50% fiber volume fraction, 2 inches fiber length) and CCF7 (150 gsm fiber tow size, 50% fiber volume fraction, 2 inches fiber length). This indicates that the 2-inch-long fibers cause the SEA of the CCF6 and CCF7 panel groups to be the least among all the CCF panel groups. It was observed in this work that the effect longer fiber lengths had on SEA was a decrease relative to the shorter fiber lengths. Therefore, it appears from this study that fiber length is the most critical material parameter determining the SEA of a composite material, with shorter fiber lengths leading to higher specific energy absorptions. As noted earlier, there is no literature available that investigates chopped carbon fibers for use in crashworthy composite materials. It would seem reasonable to set about the task of studying CCF length choices/resin choices in light of the above-reported effect of fiber length on SEA.

ACKNOWLEDGMENTS

Research was sponsored by the U.S. Department of Energy, Assistant Secretary for Energy Efficiency and Renewable Energy, Office of Transportation Technologies, Lightweight Materials Program, under contract DE-AC05-00OR22725 with UT-Battelle, LLC. The support of the Automotive Composites Consortium Energy Management Group is acknowledged.

REFERENCES

1. D. Hull, *Comp. Sci. & Tech.*, **40**, 377 (1991).
2. G.L. Farley, *Proc. 43rd American Helicopter Society Annual Forum*, St. Louis, MO, 613 (1987).
3. G.L. Farley, *J. Comp. Mater.*, **20**, 390 (1986).
4. G.L. Farley, *J. Comp. Mater.*, **17**, 267 (1983).
5. G.L. Farley, *J. Comp. Mater.*, **20**, 322 (1986).
6. G.L. Farley, *Proc. ICCM 6*, F.L. Matthews, N.C.R. Buskell, J.M. Hodgkinson, and J. Mortan, editors, 3.57 (1987).
7. P.H. Thornton and P.J. Edwards, *J. Comp. Mater.*, **16**, 521 (1982).
8. D. Hull, *Structural Crashworthiness*, N. Jones and T. Weirzbicki, editors, Butterworths, London, 118 (1983).
9. H. Hamada, S. Ramakrishna, Z. Maekawa, and M. Nakamura, *Proc. 10th Annual ASM/ESD Advanced Composite Conference*, Dearborn, MI, 511 (1994).
10. D.W. Schmuesser and L.E. Wickliffe, *J. Engng. Mat. & Tech.*, **109**, 72 (1987).
11. H. Hamada and S. Ramakrishna, *J. Thermo. Comp. Mater.*, **9**, 259 (1996).
12. G.L. Farley and R.M. Jones, *J. Comp. Mater.*, **26**, 78 (1992).
13. G.L. Farley, *J. Comp. Mater.*, **26**, 388 (1992).
14. P.H. Thornton, *J. Comp. Mater.*, **13**, 247 (1979).
15. C.H. Chiu, C.K. Lu, and C.M. Wu, *J. Comp. Mater.*, **31**, 2309 (1997).
16. C.H. Chiu, C.K. Lu, and C.M. Wu, *Proc. ICCM 10*, B.C. Whistler, editor, 4.187 (1995).

17. S. Ramakrishna, H. Hamada, Z. Maekawa, and H. Sato, *J. Thermo. Comp. Mater.*, **8**, 323 (1995).
18. I.Y. Chang and J.K. Lees, *J. Thermo. Comp. Mater.*, **1**, 277 (1988).
19. I.Y. Chang, *Comp. Sci. & Techn.*, **24**, 61 (1985).
20. H. Satoh, H. Hirakawa, Z. Maekawa, H. Hamada, M. Nakamura, and D. Hull, *38th International SAMPE Symposium, Science of Advanced Materials and Process Engineering Series*, Anaheim, CA, **38**, 952 (1993).
21. J.P. Berry, J. Blears, J.D. Grundy, R. Keale, B. Seddeon, R.P. Snowdon, and D. Hull, *Energy Absorption Composites Group Report 9*, Department of Materials Science and Metallurgy, University of Liverpool, UK (1982).
22. G.L. Farley and R.M. Jones, "Energy Absorption Capability of Composite Tubes and Beams," *NASA TM-101634, AVSCOM TR-89-B-003* (1989).
23. D. Hull, *Proc. ICCM-4*, T. Hayashi, K. Kawata, and S. Umekawa, editors, 861 (1982).
24. J.P. Berry, "Energy Absorption and Failure Mechanisms of Axially Crushed GRP Tubes," Ph.D. Thesis, University of Liverpool, UK (1984).
25. G.L. Farley, "Crash Energy Absorbing Composite Sub-floor Structure," *27th SDM Conference*, San Antonio, TX (1986).
26. G.L. Farley and R.M. Jones, *J. Comp. Mater.*, **26**, 1741 (1992).
27. P.H. Thornton, J.J. Harwood, and P. Beardmore, *Comp. Sci. & Tech.*, **24**, 275 (1985).
28. D.D. Dubey and J.A. Vizzini, *J. Comp. Mater.*, **32**, 158 (1998).
29. H. Hamada, S. Ramakrishna, Z. Maekawa, M. Nakamura, and T. Nishiwaki, *Proc. 10th Annual ASM/ESD Advanced Composite Conference*, Dearborn, MI, 523 (1994).
30. A.G. Mamalis, Y.B. Yuan, and G.L. Viegelahn, *Int. J. Vehicle Design*, **13**, 564 (1992).
31. A.H. Fairfull, "Scaling Effects in the Energy Absorption of Axially Crushed Composite Tubes," Ph.D. Thesis, University of Liverpool, UK (1986).
32. A.H. Fairfull and D. Hull, *Proc. ICCM 6*, F.L. Matthews, N.C.R. Buskell, J.M. Hodgkinson, and J. Morton, editors, 3.36 (1987).
33. G.L. Farley, "Energy Absorption Capability and Scalability of Square Cross Section Composite Tube Specimens," *U.S. Army Research and Technology Activity–AVSCOM*, 1 (1986).
34. S. Ramakrishna and H. Hamada, *Key Eng. Mater.*, **141–143**, 585 (1998).
35. S. Hanagud, J.I. Craig, P. Sriram, and W. Zhou, *J. Comp. Mater.*, **23**, 448 (1989).
36. S. Ramakrishna and D. Hull, *Comp. Sci. & Tech.*, **49**, 349 (1993).
37. S. Ramakrishna, *J. Reinf. Plast. & Comp.*, **14**, 1121 (1995).
38. P. Snowdon and D. Hull, *Proc. Fiber Reinforced Composites Conference '84*, Plastics and Rubber Institute, 5.1 (1984).
39. P.H. Thornton, W.H. Tao, and R.E. Robertson, *Advanced Composite Materials: New Development and Applications Conference Proceedings*, Detroit, MI, 489 (1991).
40. J.A. Lavoie and J. Morton, "Design and Application of a Quasistatic Crush Test Fixture for Investigating Scale Effects in Energy Absorbing Composite Plates," *NASA Contractor Report 4526* (1993).
41. D.C. Fleming and A.J. Vizzini, *Proc. American Society for Composites, 8th Technical Conference*, Cleveland, OH, 650 (1993).
42. L. Daniel, P.J. Hogg, and P.T. Curtis, *Composites: Part B*, **30**, 257 (1999).
43. G.C. Jacob, J.M. Starbuck, S. Simunovic, and J.F. Fellers, *Polym. Compos.*, **24**, 706 (2003).
44. Y.B. Yuan and G.L. Viegelahn, *Advanced Composite Materials: New Development and Applications Conference Proceedings*, Detroit, MI, 653 (1991).